Climate Dynamics (2019) 53:3971–3983
https://doi.org/10.1007/s00382-019-04764-7

Strengthened linkage between midlatitudes and Arctic in boreal winter

Xinping Xu[1] · Shengping He[1,2] · Yongqi Gao[3,4] · Tore Furevik[2] · Huijun Wang[1,4,5] · Fei Li[1,6] · Fumiaki Ogawa[2]

Received: 1 February 2018 / Accepted: 8 April 2019 / Published online: 13 April 2019

Abstract
Early studies have suggested a linkage between the surface warming over the Barents-Kara Seas and the strength of the Siberian high in boreal winter. Here, we show that the linkage is not stable, and with an apparent interdecadal change in the late-1990s. Coinciding with Arctic surface warm anomalies in recent decades (1997–2017), the Siberian high has been significantly intensified, the East Asian jet stream has expanded westward, and an apparent Rossby wave has propagated from the Arctic to East Asia, suggesting an atmospheric teleconnection between midlatitudes and Arctic. In contrast, midlatitude atmospheric circulation anomalies coinciding with Arctic surface warm anomalies were barely statistically significant during 1979–1996. The associated strong anomalous ascending/descending motions and divergent/convergent upper troposphere air masses over the Arctic-Eurasian sector seem to have favored the midlatitude-Arctic linkage during 1997–2017. We further hypothesize that Arctic mid-tropospheric warming plays a crucial role for the linkage between midlatitudes and Arctic in boreal winter. Multi-model simulations support this, and also point to internal atmospheric variability as the cause for the interdecadal shift in the strength of the midlatitude-Arctic linkage.

Keywords Linkage · Arctic warming · Siberian high · Interdecadal change · Internal variability

1 Introduction

The Arctic surface has warmed at a rate approximately twice the Northern Hemisphere average in recent decades, which is termed "Arctic amplification" (Cohen et al. 2014; Feng and Wu 2015; Francis and Vavrus 2012; Gao et al. 2015). It is generally acknowledged that the recent Arctic warming is strongly related to declining Arctic sea ice (Luo et al. 2016; Onarheim and Årthun 2017; Onarheim et al. 2015; Outten and Esau 2012; Screen et al. 2012; Smedsrud et al. 2013) and retreating snow cover (Screen and Simmonds 2010; Xu et al. 2018a). Atmospheric poleward heat and moisture transport (Chen et al. 2017; Luo et al. 2017; Screen et al. 2012; Woods and Caballero 2016), and local Arctic processes such as changes in water vapour and cloud cover (Graversen and Wang 2009) as well as sulphate aerosol and black carbon concentrations (Shindell and Faluvegi 2009), are other factors contributing to the recent Arctic warming.

Arctic surface warming has been suggested to influence winter temperature at midlatitudes, especially over Eurasia, forming the "warm Arctic-cold Eurasia" pattern (Cohen et al. 2014; Inoue et al. 2012; Kim et al. 2014; Liu et al. 2012; Luo et al. 2016; Wang and Liu 2016; Xu et al. 2018a;

✉ Shengping He
Shengping.He@uib.no

1 Collaborative Innovation Center on Forecast and Evaluation of Meteorological Disasters/Key Laboratory of Meteorological Disaster, Ministry of Education, Nanjing University of Information Science & Technology, Nanjing 210044, China

2 Geophysical Institute, University of Bergen and Bjerknes Centre for Climate Research, 5007 Bergen, Norway

3 Nansen Environmental and Remote Sensing Center and Bjerknes Centre for Climate Research, 5006 Bergen, Norway

4 Nansen-Zhu International Research Center, Institute of Atmospheric Physics, Chinese Academy of Sciences, Beijing 100029, China

5 Climate Change Research Center, Chinese Academy of Sciences, Beijing 100029, China

6 NILU-Norwegian Institute for Air Research, Kjeller 2007, Norway

Zhu et al. 2018). Overland et al. (2011) found a strengthened linkage between the warm Arctic and the midlatitude climate, manifested in the form of higher geopotential heights in the Arctic accompanied by enhanced meridional winds. A weakening of the midlatitude zonal mean flow due to reduced poleward temperature gradients associated with surface warming in the Barents-Kara Seas, contributes to the observed cooling trends across the midlatitude Eurasia (Luo et al. 2016; Outten and Esau 2012). Three possible mechanisms through which the Arctic warming could induce midlatitude weather extremes are changes in storm track, jet stream, and planetary waves (Cohen et al. 2014). In terms of the East Asian winter monsoon (EAWM) system, several studies have shown that a warm Arctic increases the geopotential height aloft, enhancing the upper-level ridge near the Urals and thus intensifying the Siberian high (Cheung et al. 2013; Cohen et al. 2014; Kug et al. 2015; Overland et al. 2015; Takaya and Nakamura 2005). However, other studies have disputed this, and attributed the winter climate change over Eurasia to internal atmospheric variability rather than to Arctic sea ice loss or Arctic warming (McCusker et al. 2016; Ogawa et al. 2018; Sorokina et al. 2016; Sun et al. 2016).

The Siberian high is one of the most distinct climate features in the Northern Hemisphere winter (He and Wang 2012; Jeong et al. 2011; Li et al. 2015). The expansion of the Siberian high is closely related to a strengthened EAWM, bringing more cold-air to East Asia (Bueh et al. 2011; He 2015; He and Wang 2013; Hu et al. 2015; Jin et al. 2016; Li and Wang 2013; Li and Yang 2010; Li et al. 2018; Wang et al. 2010; Xu et al. 2018b). The strong pressure gradient between the Siberian high and the Aleutian low gives rise to intensified northerly winds along the east flank of the Siberian high and hence causes severe winters over East Asia (Overland et al. 1999).

Planetary-scale downward motion and strong radiative cooling are thought to promote the formation and development of the Siberian high (Ding 1990; Ding and Krishnamurti 1987). More autumn Eurasian snow cover and subsequent enhanced winter surface cooling seem to have strengthened the Siberian high in recent decades, reversing a declining trend prior to the 1990s (Jeong et al. 2011; Li and Gao 2015; Panagiotopoulos et al. 2005). Much research effort has been spent in understanding the relationship between the Siberian high and changes in the Arctic properties (He and Wang 2013; Jeong et al. 2011; Jhun and Lee 2004; Li et al. 2014). For example, the negative phase of the Arctic Oscillation (AO) is linked to stronger descending motion over Siberia, exerting significant impacts on the intensity of the Siberian high (Wu and Wang 2002). Kug et al. (2015) found a relationship between surface warming in the Barents-Kara region and the strength of the Siberian high in the period 1979/1980–2013/2014, and He et al. (2016) attributed cold conditions over East Asia in January 2016 to the extreme warming in the Arctic and the concurrency of the enhanced the Siberian high.

In recent decades, there has been a striking warming trend over the Arctic (Francis and Vavrus 2015; Kug et al. 2015). As suggested by previous studies (Kumar et al. 1999; Li et al. 2014; Screen and Francis 2016), interdecadal change in background state may lead to shifts in teleconnection patterns. Notable surface warming has occurred over the Barents-Kara Seas since the late-1990s (Fig. 1a), a result of delayed ice freezing due to weaker ocean stratification in the area (Lind et al. 2018). At the same time, the Siberian high has strengthened significantly (Fig. 1b).

Motivated by the analysis of Kug et al. (2015), this study investigates the time-varying linkage between the Eurasian midlatitude circulation and Arctic climate variability

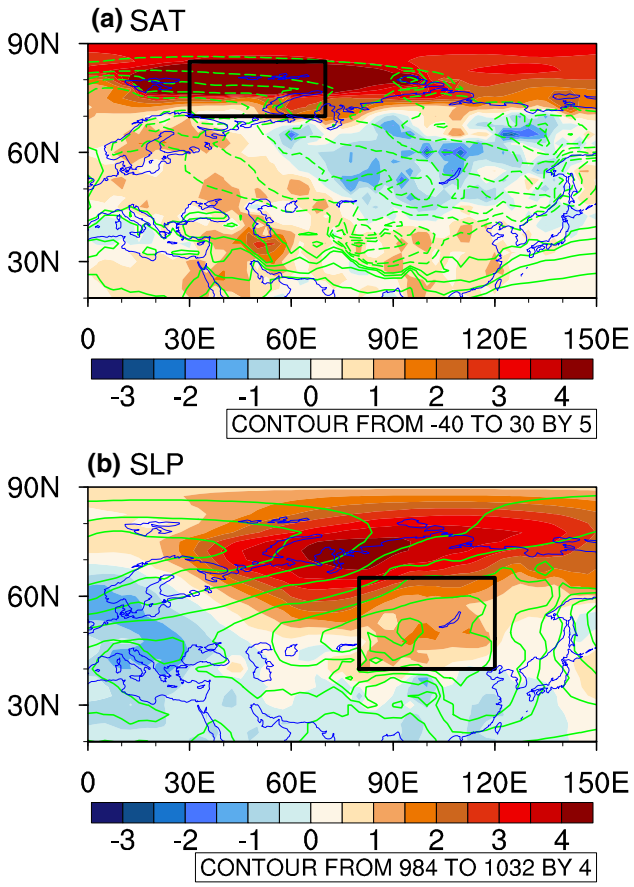

Fig. 1 **a** The climatology of winter SAT during 1979–2017 (contours) and the differences in winter SAT between 1997–2017 and 1979–1996 (shading). **b** Same as **a**, but for SLP. The boxes in **a** and **b** mark the regions where the ARTI_2m and SHI are defined, respectively

in order to gain new insights into the part of the climate system that is relevant for Arctic and midlatitude climate predictions.

2 Data and methods

The atmospheric datasets employed in this study include monthly surface air temperature (SAT), sea level pressure (SLP), air temperature, winds and vertical velocity at all levels obtained from the European Centre for Medium-Range Weather Forecasts (ECMWF) Interim Reanalysis (ERA-I) with a resolution of 2.5°×2.5° from 1979 to 2018 (Dee et al. 2011). SLP with a resolution of 5°×5° from the Met Office's Hadley Center (version of HadSLP2r) is employed to support the results derived from ERA-I reanalysis (Allan and Ansell 2006).

The Arctic surface temperature index (ARTI_2m) used in this study is defined as the area-averaged SAT over the Barents-Kara Seas (30°–70°E, 70°–85°N; the black frame in Fig. 1a), and the Arctic mid-tropospheric temperature index (ARTI_500) is defined as the area-averaged temperature at 500 hPa over the same area. The Siberian high index (SHI) is defined as the area-averaged SLP in the region of 80°–120°E, 40°–65°N (the black frame in Fig. 1b) (Jeong et al. 2011). A winter of a particular year refers to December that year and January and February next year. To focus on the interannual variability, all data are linearly de-trended before the regression and correlation analyses.

We utilize four uncoupled (atmosphere-only) climate models, each forced by daily-varying SST and sea ice in the period of 1982–2014 (Ogawa et al. 2018). The models are the Community Atmosphere Model, version 4 (CAM4, 0.9°×1.25° with 26 vertical levels up to 3 hPa) (Neale et al. 2013), the Whole Atmosphere Community Climate Model (WACCM, 0.9°×1.25° with 66 vertical levels up to 0.000006 hPa) (Marsh et al. 2013), and the Integrated Forecast System (IFS, T255 with 91 vertical levels up to 0.01 hPa) (Balsamo et al. 2009) with twenty independent runs each, and the fourth generation atmospheric general circulation model developed at the Institute of Atmospheric Physics, Chinese Academy of Science (IAP4, 1.4°×1.4° with 26 vertical levels up to 10 hPa) (Dong et al. 2012) with ten independent runs. All experiments are forced with the Coupled Model Intercomparison Project Phase 5 (CMIP 5) historical forcing for 1982–2005 and Representative Concentration Pathway 8.5 scenarios (RCP 8.5) for 2006–2014. The surface boundary forcing involves observed daily SST and sea ice taken from NOAA OISST (Reynolds et al. 2007).

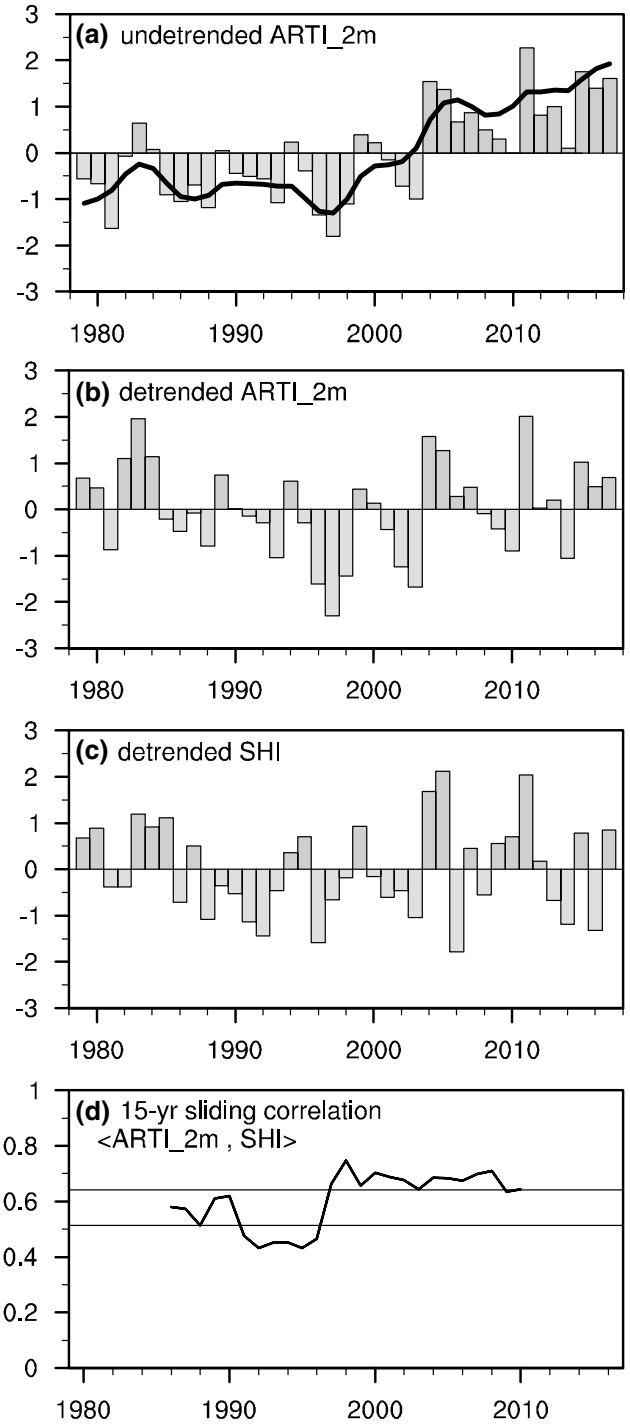

Fig. 2 Normalized time series of **a** undetrended winter ARTI_2m (bars) and its 7-year moving averages (solid lines) and detrended winter **b** ARTI_2m and **c** SHI during 1979–2017. **d** The 15-year sliding correlation coefficients between the detrended ARTI_2m and SHI during 1979–2017. The solid lines indicate the values significant at the 95% and 99% confidence levels

3 Interdecadal variation in the relationship between midlatitude atmospheric circulation anomalies and Arctic temperature variability

Figure 2a shows the temporal evolutions of the undetrended winter ARTI_2m and its 7-year running mean during 1979–2017. One of the most striking features is the interdecadal transition of Arctic surface temperature anomaly, with a steep warming trend after the late-1990s as pointed out by Kug et al. (2015) and also found in the water below (Lind et al. 2018). The linkage between Eurasian midlatitude climate and Arctic surface temperature variability (Kug et al. 2015), with an enhanced Siberian high and an anomalous anticyclonic circulation in western Russia associated with warm anomalies in the Barents-Kara Seas, is indicated by the significant positive correlations between the ARTI_2m and Siberian high pressure (Fig. 3a, d). The strengthened linkage between Arctic surface warming and midlatitude atmospheric circulation around the late-1990s (Fig. 2d) is investigated in more detail in the following analysis.

Winter SLP and UV850 are regressed onto the ARTI_2m for the two periods 1979–1996 and 1997–2017 (Fig. 3b, c). During 1979–1996, there are positive but mostly insignificant SLP anomalies largely confined to western Siberia reaching 1.5 hPa (Fig. 3b; shading). Accordingly, at 850 hPa, the anomalous anticyclonic flow over western Siberia-eastern Europe for 1979–2017 (Fig. 3a; vectors) is replaced by anomalous southeast and east airflows on the west of the Lake Baikal (Fig. 3b; vectors). It seems that changes in Arctic surface temperature have a weaker and less significant relationship with the midlatitude atmospheric circulation during 1979–1996, relative to that during 1979–2017. For the period 1997–2017, a significant anomalous high pressure is located over the east of the Ural Mountains reaching 3 hPa (Fig. 3c; shading). Also, a significant anticyclonic anomaly appears over northern Eurasia (Fig. 3c; vectors). Comparison of circulation anomalies between the two periods demonstrates the strengthening of the linkage between the Arctic surface temperature and the Siberian high in the latter period. The results based on ERA-I reanalysis (Fig. 3a–c) resemble closely those based on observations from Hadley Center (Fig. 3d–f), supporting the robustness of the strengthened midlatitude-Arctic linkage.

Generally, the Siberian high is closely linked to upper-tropospheric circulation (Jhun and Lee 2004; Panagiotopoulos et al. 2005; Yang et al. 2002). The 300 hPa zonal wind

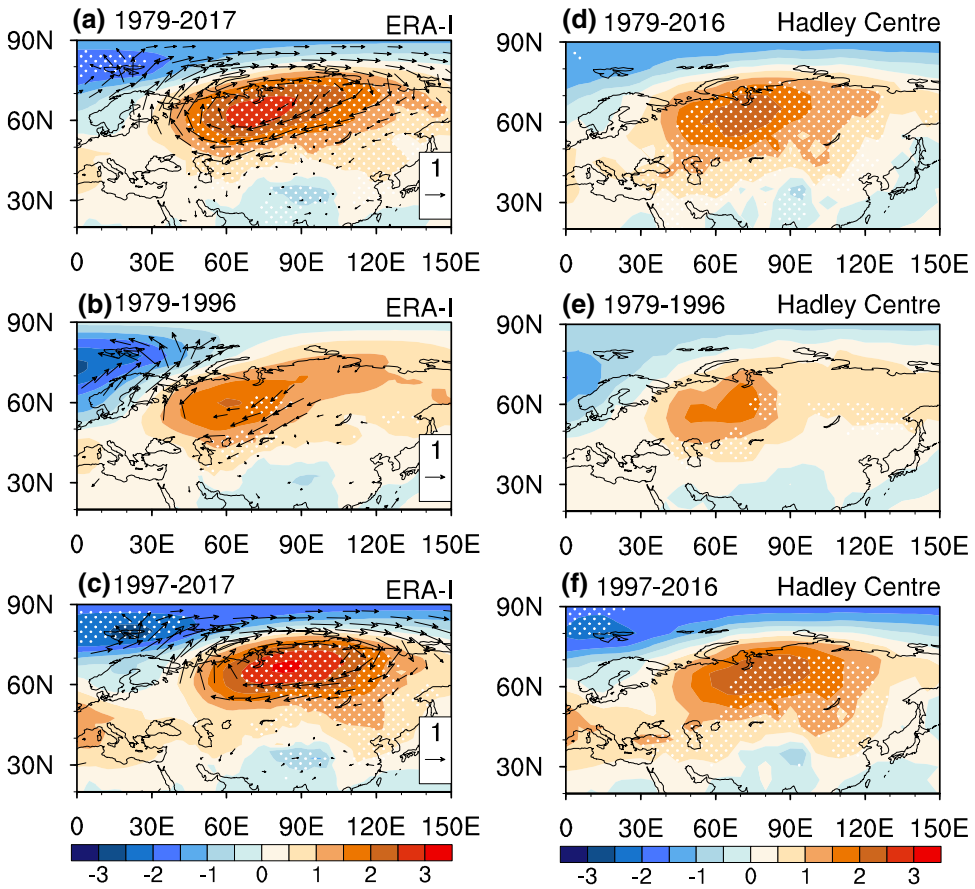

Fig. 3 **a** Regressions of winter SLP (shading) and UV850 (vectors) with respect to the ARTI_2m derived from ERA-I reanalysis data during **a** 1979–2017, **b** 1979–1996, and **c** 1997–2017, respectively. **d–f** Same as **a–c**, but for SLP derived from Met Office's Hadley Centre data during **d** 1979–2016, **e** 1979–1996, and **f** 1997–2016, respectively. Areas with correlations exceeding the 95% confidence level are dotted. The vector winds are above the 95% confidence level

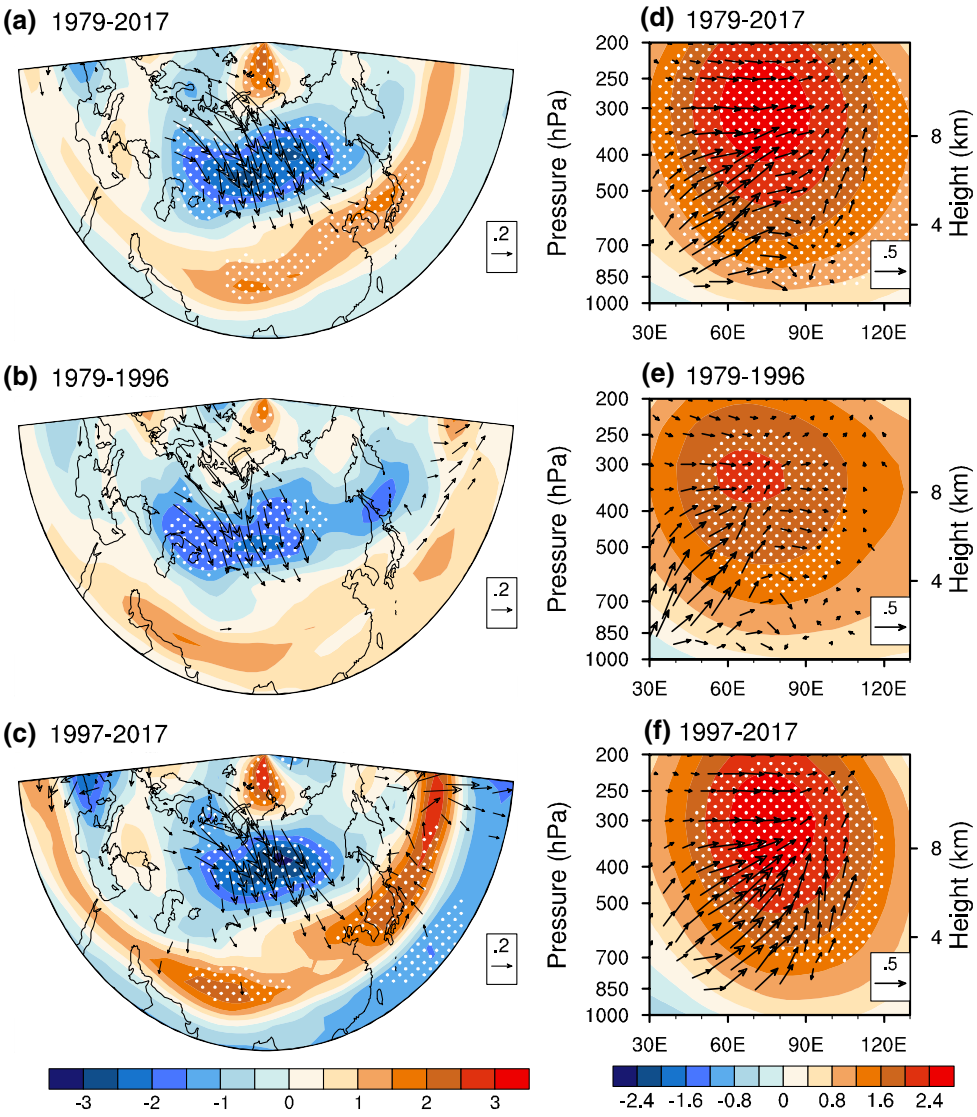

Fig. 4 Regressions of winter 300 hPa zonal wind (shading) and wave activity flux (vectors; $m^2\ s^{-2}$) with respect to the ARTI_2m during **a** 1979–2017, **b** 1979–1996, and **c** 1997–2017, respectively. **d**–**f** Same as **a**–**c**, but for quasi-geostrophic streamfunction (shading; $10^6\ m^2\ s^{-1}$) and wave activity flux (vectors; $m^2\ s^{-2}$, vertical component is multiplied by 100) averaged along 65°–90°N. Areas with correlations exceeding the 95% confidence level are dotted

(shading) and wave activity flux (vectors) (computed according to Takaya and Nakamura 2001) are therefore regressed onto the ARTI_2m during 1979–2017, 1979–1996, and 1997–2017 (Fig. 4a–c). The prevailing westerly winds encircling the Arctic show a remarkable weakening during the Arctic surface warm years for all three periods (Fig. 4a–c; shading), which might be related to the decreased meridional temperature gradient associated with Arctic warming through the thermal wind relation (Francis and Vavrus 2015; Overland et al. 2015). The magnitude of the anomalous easterly winds during 1997–2017 is slightly larger than that for 1979–1996 (Fig. 4b, c; shading). Meanwhile, there is an accelerated and westward-extended East Asian jet stream after the late-1990s (Fig. 4c; shading). The "negative-positive" anomaly structure of the 300 hPa zonal wind oriented north-south over East Asia-western Pacific sector is closely connected with the amplifying of the Siberian high (Jhun and Lee 2004). Downstream-propagating wave trains, which are initiated by the augmented ridge related to Arctic amplification and can be expressed by the wave activity flux, could induce cold spells over East Asia (Kug et al. 2015; Mori et al. 2014). Apparently, upward-directed wave activity flux associated with warm conditions in the Arctic surface is observed during all three periods (Fig. 4d–f; vectors). The eastward propagation of upper-level planetary-scale waves only extends to high-latitude Eurasia during 1979–1996 while reaches East Asia after the late-1990s (Fig. 4a–c; vectors), promoting the linkage between the midlatitudes and the Arctic. The presence of the enhanced and upstream-extended East Asian jet stream coincides with the southeastward-propagating wave trains after the late-1990s (Li et al. 2014).

In the conventional description, the intensity of the Siberian high strongly depends on the behavior of the descending motion in the Siberian region (Ding 1990). In order to investigate the changes in the dynamic processes associated

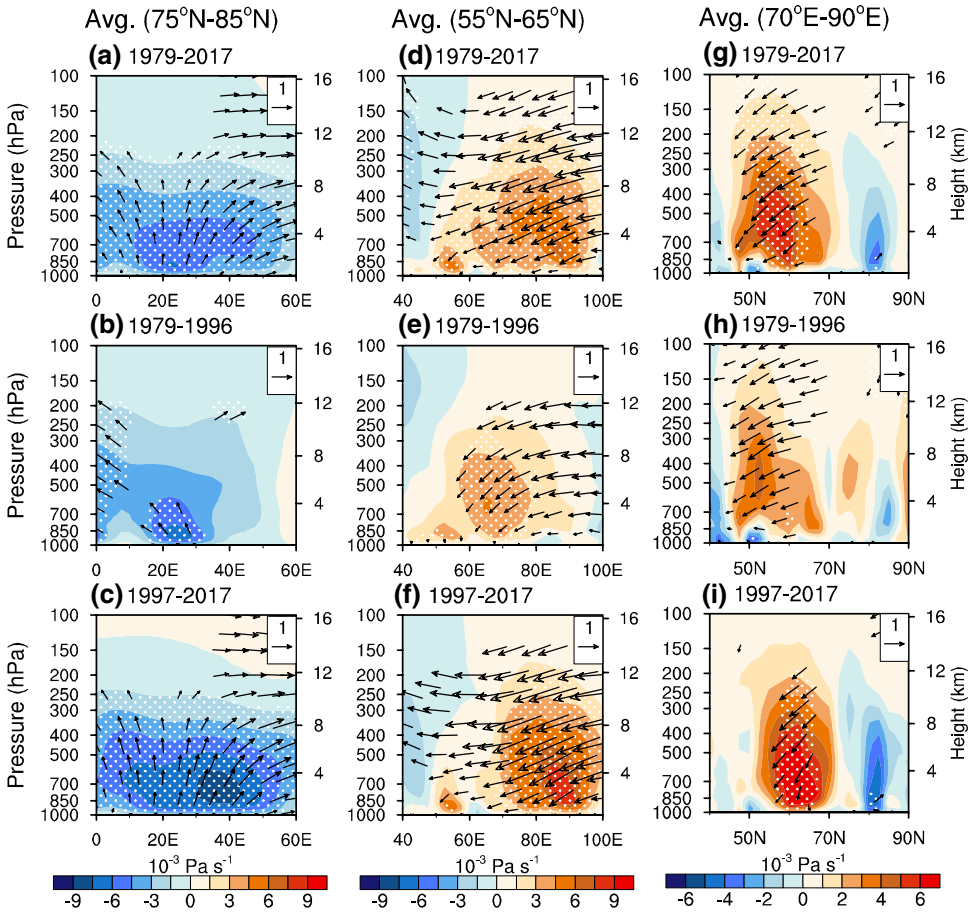

Fig. 5 Regressions of winter vertical circulation (vectors; m s^{-1}) and vertical velocity (shading; 10^{-3} Pa s^{-1}) anomalies averaged along 75°–85°N with respect to the ARTI_2m during **a** 1979–2017, **b** 1979–1996, and **c** 1997–2017, respectively. **d**–**f** And **g**–**i** same as **a**–**c**, but averaged along 55°–65°N and 70°–90°E, respectively. Areas with correlations exceeding the 95% confidence level are dotted. The vector winds are above the 95% confidence level

with the Arctic temperature-Siberian high relationship, the vertical circulation is regressed upon the ARTI_2m (Fig. 5). Associated with the surface warm conditions in the Barents-Kara Seas during 1979–2017, there is an anomalous ascending motion tilting eastward with altitude (75°–85°N) (Fig. 5a) and an anomalous descending motion over Siberia (55°–65°N) (Fig. 5d). The averaging range for vertical sections is selected according to the significant vertical velocity values at 500 hPa (figure not shown). In latitude-height plane, the southward airflow to the east of the Barents-Kara Seas might link the anomalous ascending motions in the Arctic and descending motion over Siberia due to the Coriolis force (70°–90°E) (Fig. 5g). Therefore, we speculate that it forms a plausible atmospheric bridge between the midlatitudes and the Arctic, through which the Arctic surface temperature change is linked to the intensity of the Siberian high. Comparing 1979–1996 with 1997–2017, striking differences are seen in Siberia and the Arctic. The anomalous ascending motion over the Arctic and the subsidence over Siberia are much stronger in the latter period (Fig. 5c vs. b, f vs. e). Furthermore, the anomalous northerly from the Arctic to Siberia is more significant after the late-1990s (Fig. 5i vs. h), concurrent with pronounced anomalous subsidence at midlatitudes (around 60°N) where the Siberian high is located (Fig. 5i). The notable difference in the dynamic processes associated with Arctic surface warm anomalies in the two periods means that the atmospheric bridge is more likely to be present after the late-1990s.

To further explore this, we regress the divergence of the wind field at both 1000 hPa and 300 hPa with respect to the ARTI_2m during the three periods (Fig. 6). A dynamically consistent structure associated with Arctic surface warm anomalies is observed during 1979–2017, with significant anomalous convergence (divergence) in the lower troposphere and anomalous divergence (convergence) in the upper troposphere over the Arctic (Eurasia) (Fig. 6a, d). This leads to anomalous downward motion in Siberia and the development of the Siberian high (Ding 1990). Accordingly, the atmospheric bridge can be physically understood in the following way. Significant Arctic surface warm anomalies lead to stretching of air column, higher pressure and divergence aloft, which in turn causes lower pressure and convergence close to surface. The anomalous divergence aloft favors a large-scale upper-tropospheric mass convergence to the east and descending motion over Siberia, leading to lower-level divergent airflow and enhancement of the Siberian high. The lower-level divergence in turn favors the Arctic mass convergence, thereby causing an atmospheric bridge between the

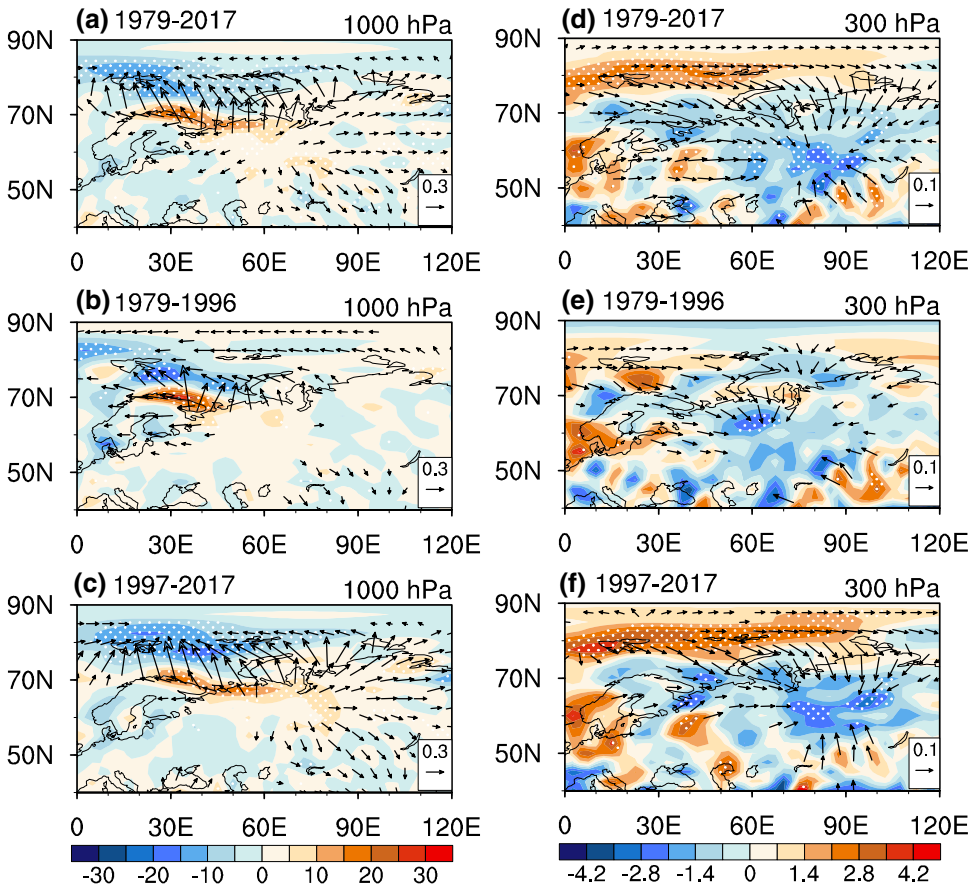

Fig. 6 Regressions of winter 1000 hPa divergence (shading; 10^{-7} s^{-1}) and divergent winds (vectors; m s^{-1}) with respect to the ARTI_2m during **a** 1979–2017, **b** 1979–1996, and **c** 1997–2017, respectively. **d**–**f** Same as **a**–**c**, but for 300 hPa. Areas with correlations exceeding the 95% confidence level are dotted. The vector winds are above the 95% confidence level

Barents-Kara Seas and Siberia. It is apparent that the lower-level convergence (divergence) and upper-level divergence (convergence) anomalies over the Arctic (Eurasia) associated with Arctic surface warm anomalies strengthen after the late-1990s (Fig. 6c vs. b, f vs. e), illustrating the intensified midlatitude-Arctic linkage.

4 Discussion on the interdecadal change in the midlatitude-Arctic linkage

Arctic warming has a maximum at the surface and extends to the upper troposphere, decreasing with height (Screen and Simmonds 2010). Cohen et al. (2018) pointed out that Arctic tropospheric warming is associated with more extreme winter weather in the United States. Amplified Arctic warming throughout the troposphere after the late-1990s (Figure not shown) motivates us to consider the relationship between the variability of the Arctic mid-tropospheric temperature and change in the midlatitude-Arctic linkage. Figure 7a shows the normalized time series of the detrended ARTI_500. Amplitudes are enhanced after the late-1990s, with standard deviation increasing from 0.87 to 1.12 between 1979–1996 and 1997–2017. Also the sliding correlation between the ARTI_500 and SHI becomes stronger after the late-1990s (Fig. 7b), which is even more robust than change in the relationship between the ARTI_2m and SHI (Fig. 2d).

To investigate the potential role of Arctic mid-tropospheric temperature, we calculate the sliding correlation between the residual ARTI_2m (where the ARTI_500 effect has been removed using linear regression) and SHI. It turns out that the Arctic temperature-Siberian high relationship becomes statistically insignificant when the mid-tropospheric temperature variability is removed (Fig. 7c). Previous study revealed that the anomalous Siberian high is concurrent with significant positive anomalies of the surface temperature over the Barents-Kara Seas (Kug et al. 2015), as shown in Fig. 3a. Note that the surface temperature anomalies over the Barents-Kara Seas are significantly positive (Fig. 8a) while there is no significant intensified Siberian high (Fig. 8b). Thus it seems that the relationship between the Arctic temperature and the Siberian high might be determined by the Arctic mid-tropospheric temperature and not the surface temperatures per se.

Then, is it possible that the Arctic surface warm anomalies are accompanied with stronger Arctic mid-tropospheric warm anomalies after the late-1990s? In Fig. 9, the zonally averaged winter air temperature and zonal wind anomalies over the region of 30°–70°E in the warmer Arctic surface years (ARTI_2m ≥ 0.8) during 1979–1996 and 1997–2017

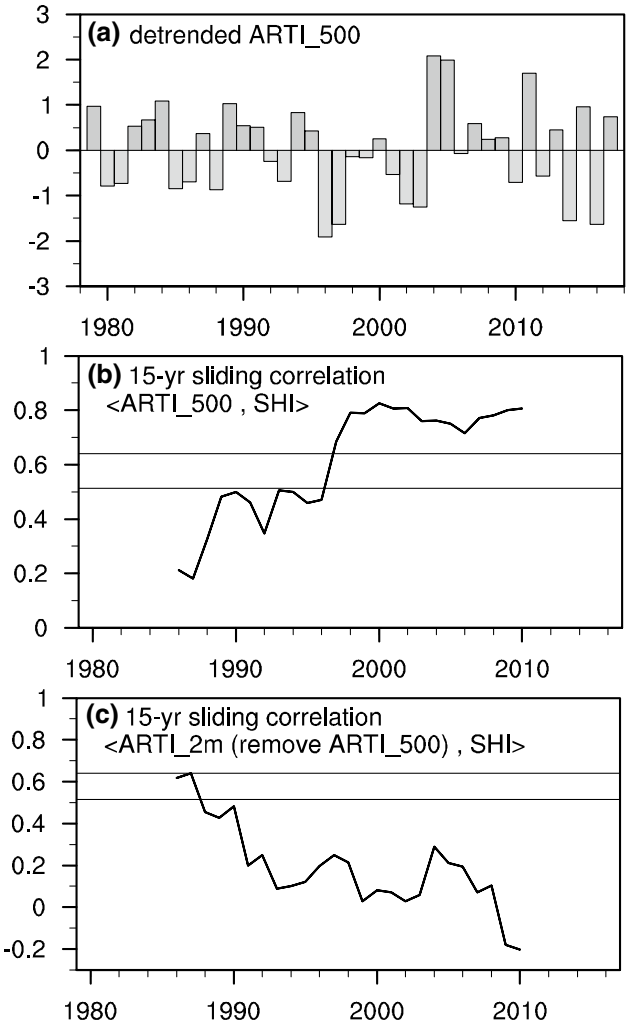

Fig. 7 **a** Normalized time series of detrended winter ARTI_500 during 1979–2017. **b** The 15-year sliding correlation coefficients between the detrended ARTI_500 and SHI during 1979–2017. The solid lines indicate the values significant at the 95% and 99% confidence levels. **c** Same as Fig. 2d, but for the residual winter ARTI_2m after linearly removing the ARTI_500

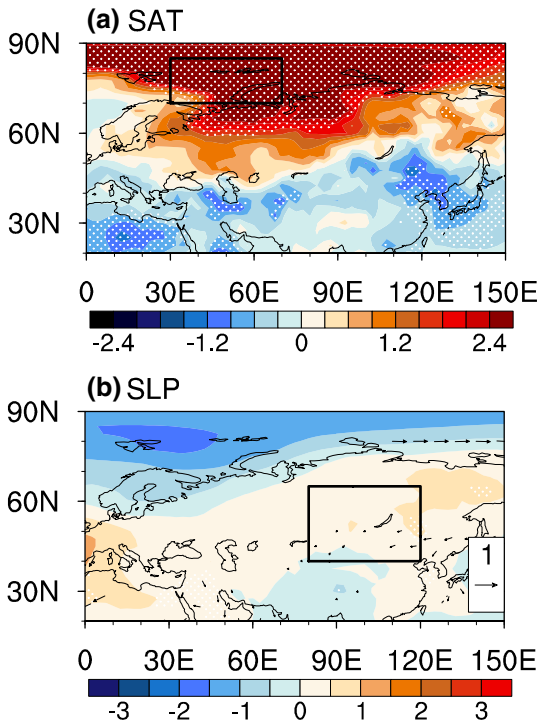

Fig. 8 **a** Regressions of winter SAT with respect to the residual ARTI_2m during 1979–2017. **b** Same as **a**, but for SLP (shading) and UV850 (vectors). Areas with correlations exceeding the 95% confidence level are dotted. The vector winds are above the 95% confidence level

and their difference (1997–2017 minus 1979–1996) are presented. Apparently, there are significant upper tropospheric warm anomalies in the warmer Arctic surface years during 1997–2017 (Fig. 9b; shading), while there are only significant lower tropospheric warm anomalies during 1979–1996 (Fig. 9a; shading). That is, Arctic surface warm anomalies are significantly associated with mid-tropospheric warm anomalies after the late-1990s. Also, Arctic mid-tropospheric temperature anomaly in the latter period can reach up to 1.8 °C (Fig. 9b; shading), approximately twice the values during 1979–1996 (Fig. 9a; shading). In other words, even if the detrended Arctic surface temperature anomalies are comparable between 1979–1996 and 1997–2017 (around 2.4 °C), the associated Arctic mid-tropospheric warm anomaly after the late-1990s is larger by ~1.2 °C (Fig. 9c; shading). Meanwhile, there is a significant weakening of the midlatitude jet stream in the warmer Arctic surface years after the late 1990s with larger amplitude (~ -2.5 m s^{-1}) than during 1979–1996 (~ -1.5 m s^{-1}) (Fig. 9; contours). We therefore hypothesize that Arctic mid-tropospheric warming after the late 1990s might be associated with the interdecadal strengthened midlatitude-Arctic linkage.

It is difficult to determine it is the Arctic mid-tropospheric warming causes the interdecadal shift in the midlatitude-Arctic linkage or otherwise. Actually, there is no consensus among scientific communities about the causality between midlatitude circulations and Arctic warming (Chen et al. 2017; Liu et al. 2012; Mori et al. 2014; Woods and Caballero 2016). They could be caused by internal atmospheric variability or driven by some external forcing. We therefore apply multi-model simulations (Ogawa et al. 2018) to search for the cause for the interdecadal change in the Arctic tropospheric temperature and the midlatitude-Arctic linkage.

Arctic warming in the ensemble-mean of climate model simulations is mainly confined to near-surface (Ogawa et al. 2018; Screen et al. 2018). However, in the individual ensembles there are members having shallow Arctic warming and others where the warming spans from surface to mid- and even to upper troposphere. Specifically, eleven

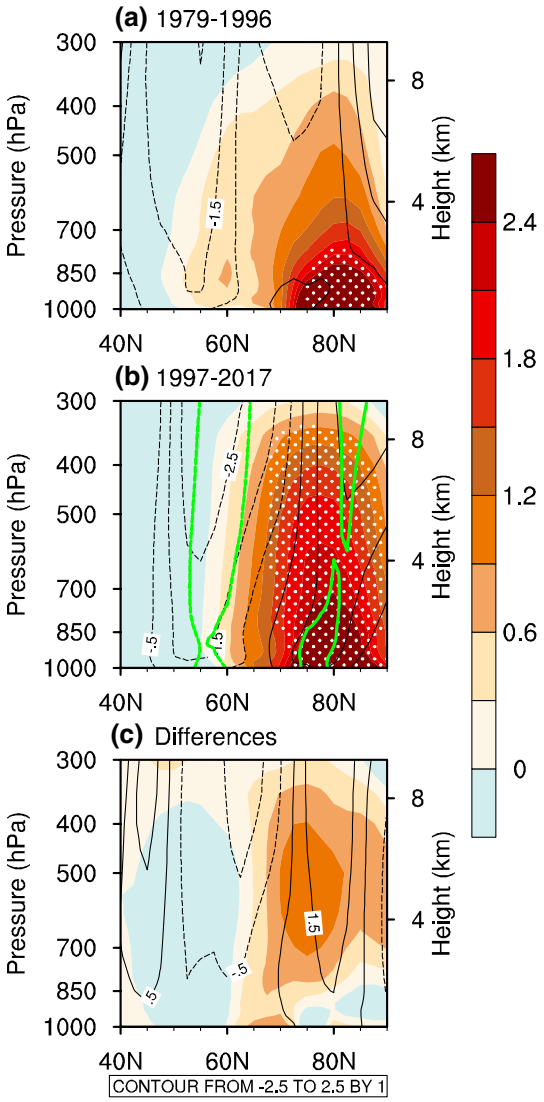

Fig. 9 Winter temperature (shading) and zonal wind (black contours) anomalies averaged along 30°–70°E in the warmer Arctic surface years (ARTI_2m ≥ 0.8) during **a** 1979–1996 and **b** 1997–2017 and **c** their difference (1997–2017 minus 1979–1996); the anomalies are relative to the climatology of 1979–2017. **a**, **b** Regions with white dots (green contours) indicate that the temperature (zonal wind) anomalies are significant at the 95% confidence level

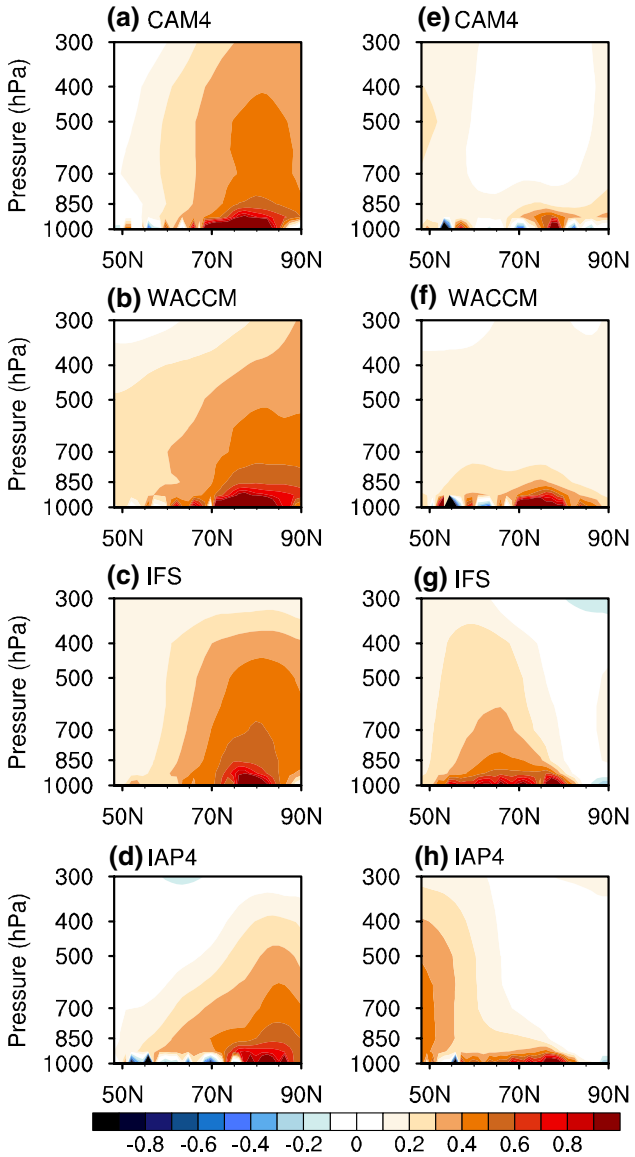

Fig. 10 **a**–**d** The simulated winter temperature trend averaged along 30°–70°E during 1982–2013 from the ensembles that simulate the Arctic middle tropospheric warming trend in **a** CAM4, **b** WACCM, **c** IFS, and **d** IAP4, respectively. **e**–**h** Same as **a**–**d**, but from the rest ensembles that simulate the Arctic warming trend confined to near-surface

members from CAM4, fourteen members from WACCM, fifteen members from IFS, and two members from IAP4 successfully simulate Arctic mid-tropospheric warming (identified by the threshold above 0.2 °C per decade in 500 hPa warming trend over the Barents-Kara Seas). These members are selected. For these selected ensembles' mean in each model, it is apparent that the simulated Arctic warming extends across the mid-troposphere with maximum values at the surface (Fig. 10a–d) (referred as the category of Arctic mid-tropospheric warming); while in the rest ensembles, the simulated Arctic warming is confined to near-surface (Fig. 10e–h) (referred as the category of Arctic surface warming). All models are forced with the same SST and sea ice but different initial conditions. The different vertical structures of the warming in the same model suggest that internal stochastic atmospheric variability might play an important role in the observed Arctic mid-tropospheric warming. Since the ensemble members have different warming structures, we next test the models for the midlatitude-Arctic linkage.

Figure 11 displays the winter SLP anomalies regressed onto the ARTI_2m in the two categories of Arctic warming.

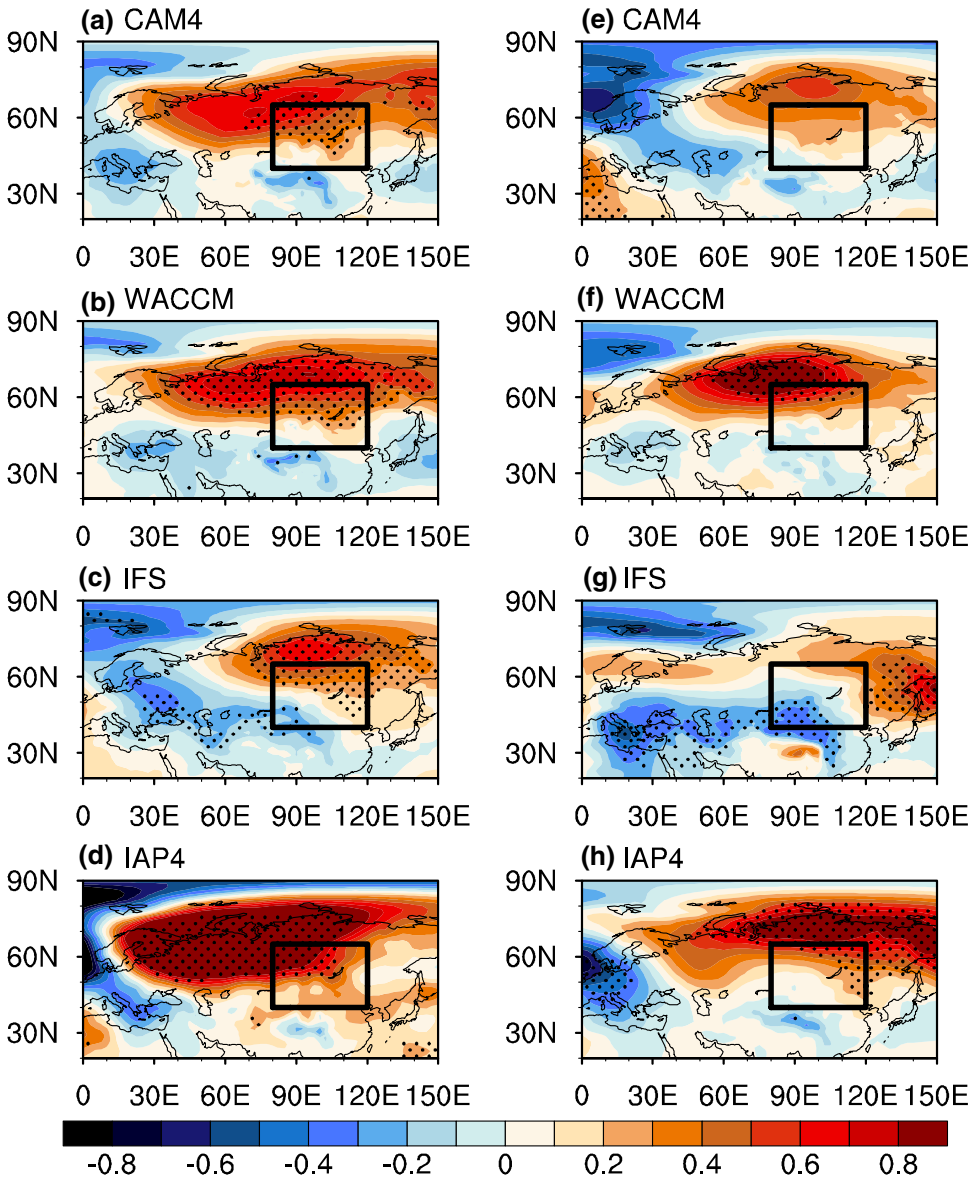

Fig. 11 **a**–**d** The simulated regressions of winter SLP with respect to the ARTI_2m during 1982–2013 from the ensembles that simulate the Arctic middle tropospheric warming trend in **a** CAM4, **b** WACCM, **c** IFS, and **d** IAP4, respectively. **e**–**h** Same as **a**–**d**, but from the rest ensembles that simulate the Arctic warming trend confined to near-surface. Areas with correlations exceeding the 90% confidence level are dotted. The box marks the region where the SHI is defined

Compared with the ensemble members showing shallow Arctic warming (Fig. 11e–h), the winter Siberian SLP anomalies associated with ARTI_2m are uniformly stronger and more significant in the ensemble members where the Arctic warming reaches mid-troposphere (Fig. 11a–d). Quantitatively, the Siberian area-averaged SLP anomalies (unit: hPa; black frame in Fig. 11) in the category of Arctic mid-tropospheric warming are 0.32, 0.31, 0.16, and 0.49 in each model, which are correspondingly stronger than those (0.19, 0.27, − 0.02, and 0.25) associated with Arctic surface warming. Thus, the multi-model simulations support our hypothesis that the interdecadal strengthened midlatitude-Arctic linkage is associated with Arctic mid-tropospheric warming and suggest that the internal atmospheric variability plays an important role in the interdecadal change. This is also consistent with the conclusion by Sung et al. (2018) that the interdecadal variability of the warm Arctic-cold Eurasian pattern in the twentieth century might be attributed to the internal atmospheric variability.

With respect to the contentious topic, some discussion is further given. It might be worth noting that the change of the poleward temperature gradient and the midlatitude zonal wind is not apparent when Arctic warming is confined to near-surface, which is much more dominant when Arctic warming extends from surface to the mid-troposphere (figure not shown). The warm Arctic mid-troposphere after the late-1990s, which might be due to the internal atmospheric variability as suggested by our model simulations and previous studies (Graversen et al. 2008; Lee et al. 2017), may contribute to the weakening of the zonal wind based on the thermal wind balance and the intensified linkage between Arctic warming and the midlatitude climate (Liu et al. 2012;

Vavrus 2018; Yao et al. 2017). The possible mechanisms implied here are currently under investigation in a companion study.

5 Conclusions

Previous study has shown that surface warming over the Barents-Kara Seas in boreal winter is generally associated with an intensified Siberian high (Kug et al. 2015). Based on the reanalysis data, this study explores the strength of the midlatitude-Arctic linkage. The correlations between the Arctic surface temperature and the Siberian high show an apparent intensification around late-1990s. After this, the warmer-than-normal Arctic is generally concurrent with significant positive SLP anomalies stretching from the Barents-Kara Seas to East Asia, indicating a stronger-than-normal Siberian high. Moreover, the westward-extended East Asian jet stream occurs in conjunction with the southeastward propagation of Rossby waves from the Arctic to East Asia, displaying an apparent midlatitude-Arctic linkage. Anomalous ascending/descending motions and upper tropospheric divergence/convergence anomalies over the Arctic-Eurasian sector indicate a potential dynamical atmospheric bridge that favors the midlatitude-Arctic linkage after the late-1990s. By contrast, Eurasian midlatitude atmospheric circulation anomalies barely correlate with Arctic surface warm anomalies in the decades before late-1990s.

There has been a rapid tropospheric warming trend over the Arctic after the late-1990s, with increased Arctic mid-tropospheric temperature variability. Further analysis shows that no significant intensified Siberian high is observed when the Arctic warm anomalies are confined to near-surface without significant warm anomalies in the mid-troposphere. That is, the interannual relationship between the Arctic surface temperature and the Siberian high might be determined by the variability of the Arctic mid-tropospheric temperature. Moreover, the Arctic surface warm anomalies are accompanied with significantly stronger Arctic mid-tropospheric warm anomalies after the late-1990s. We therefore hypothesize that the interdecadal Arctic mid-tropospheric warming might be associated with the interdecadal intensified midlatitude-Arctic linkage.

Simulations from multi-model ensembles forced with observed SST and sea ice also support the concurrency of Arctic mid-tropospheric warming and the strengthened midlatitude-Arctic linkage. While the multi-model ensemble mean displays a shallow Arctic warming and no apparent anomalous atmospheric circulation at midlatitudes (Ogawa et al. 2018), some individual ensemble members reproduce the observed Arctic warming across the mid-troposphere. It is found that the category of Arctic tropospheric warming does display a significant Arctic temperature-Siberian high relationship, while it is much weaker in the category of Arctic surface warming. The analysis from the reanalysis dataset and the multi-model simulations does not emphasize the effect of the Arctic mid-tropospheric warming or the Siberian high on the interdecadal shift in the midlatitude-Arctic linkage, but shows robust evidence for the concurrency of the Arctic mid-tropospheric warming and the strengthened midlatitude-Arctic linkage. The causal relationship is currently under investigation in a companion study. It should also be pointed out that all the models in this study are forced with the same observed SST and sea ice but different initial conditions, suggesting the potential contribution of the internal atmospheric variability to Arctic mid-tropospheric warming and the interdecadal shift in the midlatitude-Arctic linkage.

Acknowledgements This research was supported by the National Key R&D Program of China (2016YFA0600703), the CONNECTED supported by UTFORSK Partnership Program (UTF-2016-long-term/10030), the Research Council of Norway supported project SNOWGLACE (244166/E10) and InterDec (260393), the National Natural Science Foundation of China (Grants 41875118, 41505073, 41605059, 41421004, and 41790472), the Young Talent Support Program by China Association for Science and Technology (Grant 2016QNRC001), the Postgraduate Research & Practice Innovation Program of Jiangsu Province (KYCX18_0997), the funding of Jiangsu innovation and entrepreneurship team, and the Priority Academic Program Development (PAPD) of Jiangsu Higher Education Institutions.

References

Allan R, Ansell T (2006) A new globally-complete monthly historical gridded mean sea level pressure data set (HadSLP2): 1850–2004. J Clim 19:5816–5841

Balsamo G, Viterbo P, Beljaars A, Hurk BVD, Hirschi M, Betts AK, Scipal K (2009) A revised hydrology for the ECMWF model: verification from field site to terrestrial water storage and impact in the Integrated Forecast System. J Hydrometeorol 10:623–643

Bueh C, Fu X, Xie Z (2011) Large-scale circulation features typical of wintertime extensive and persistent low temperature events in China. Atmos Ocean Sci Lett 4:235–241

Chen X, Luo D, Feldstein SB, Lee S (2017) Impact of winter Ural blocking on Arctic sea ice: short-time variability. J Clim 31:2267–2282

Cheung HN, Zhou W, Shao Y, Chen W, Mok HY, Wu MC (2013) Observational climatology and characteristics of wintertime atmospheric blocking over Ural-Siberia. Clim Dyn 41:63–79

Cohen J et al (2014) Recent Arctic amplification and extreme mid-latitude weather. Nat Geosci 7:627–637

Cohen J, Pfeiffer K, Francis JA (2018) Warm Arctic episodes linked with increased frequency of extreme winter weather in the United States. Nat Commun 9:869

Dee DP et al (2011) The ERA-Interim reanalysis: configuration and performance of the data assimilation system. Q J R Meteorol Soc 137:553–597

Ding Y (1990) Build-up, air mass transformation and propagation of Siberian high and its relations to cold surge in East Asia. Meteorol Atmos Phys 44:281–292

Ding Y, Krishnamurti TN (1987) Heat budget of the Siberian high and the winter monsoon. Mon Weather Rev 115:2428–2449

Dong X, Xue F, Zhang H, Zeng Q (2012) Evaluation of surface air temperature change over China and the globe during the twentieth century in IAP AGCM4.0. Atmos Ocean Sci Lett 5:435–438
Feng C, Wu B (2015) Enhancement of winter Arctic warming by the Siberian high over the past decade. Atmos Ocean Sci Lett 8:257–263
Francis JA, Vavrus SJ (2012) Evidence linking Arctic amplification to extreme weather in mid-latitudes. Geophys Res Lett 39:L06801
Francis JA, Vavrus SJ (2015) Evidence for a wavier jet stream in response to rapid Arctic warming. Environ Res Lett 10:014005
Gao Y et al (2015) Arctic sea ice and Eurasian climate: a review. Adv Atmos Sci 32:92–114
Graversen RG, Wang M (2009) Polar amplification in a coupled climate model with locked albedo. Clim Dyn 33:629–643
Graversen RG, Mauritsen T, Tjernström M, Källén E, Svensson G (2008) Vertical structure of recent Arctic warming. Nature 451:53–56
He S (2015) Asymmetry in the Arctic Oscillation teleconnection with January cold extremes in Northeast China. Atmos Ocean Sci Lett 8:386–391
He S, Wang H (2012) An integrated East Asian winter monsoon index and its interannual variability. Chin J Atmos Sci 36:523–538
He S, Wang H (2013) Impact of the November/December Arctic Oscillation on the following January temperature in East Asia. J Geophys Res 118:12981–12998
He S, Wang H, Xu X, Li J (2016) Impact of Arctic warming and the super El Nino in winter 2015/2016 on the East Asian climate anomaly. Trans Atmos Sci 39:735–743
Hu C, Yang S, Wu Q (2015) An optimal index for measuring the effect of East Asian winter monsoon on China winter temperature. Clim Dyn 45:2571–2589
Inoue J, Hori ME, Takaya K (2012) The role of Barents sea ice in the wintertime cyclone track and emergence of a warm-Arctic cold-Siberian anomaly. J Clim 25:2561–2568
Jeong JH, Ou T, Linderholm HW, Kim BM, Kim SJ, Kug JS, Chen D (2011) Recent recovery of the Siberian high intensity. J Geophys Res 116:D23102
Jhun JG, Lee EJ (2004) A new East Asian winter monsoon index and associated characteristics of the winter monsoon. J Clim 17:711–726
Jin C, Zhou T, Guo Z, Wu B, Chen X (2016) Improved simulation of the East Asian winter monsoon interannual variation by IAP/LASG AGCMs. Atmos Ocean Sci Lett 9:204–210
Kim BM et al (2014) Weakening of the stratospheric polar vortex by Arctic sea-ice loss. Nat Commun 5:4646
Kug JS, Jeong JH, Jang YS, Kim BM, Folland CK, Min SK, Son SW (2015) Two distinct influences of Arctic warming on cold winters over North America and East Asia. Nat Geosci 8:759–762
Kumar KK, Rajagopalan B, Cane MA (1999) On the weakening relationship between the Indian monsoon and ENSO. Science 284:2156–2159
Lee HJ et al (2017) Impact of poleward moisture transport from the North Pacific on the acceleration of sea ice loss in the Arctic since 2002. J Clim 30:6757–6769
Li F, Gao Y (2015) The project Siberian high in CMIP5 models. Atmos Ocean Sci Lett 8:179–184
Li F, Wang H (2013) Autumn sea ice cover, winter Northern Hemisphere annular mode, and winter precipitation in Eurasia. J Clim 26:3968–3981
Li Y, Yang S (2010) A dynamical index for the East Asian winter monsoon. J Clim 23:4255–4262
Li F, Wang H, Gao Y (2014) On the strengthened relationship between the East Asian winter monsoon and Arctic Oscillation: a comparison of 1950–70 and 1983–2012. J Clim 27:5075–5091
Li F, Wang H, Gao Y (2015) Change in sea ice cover is responsible for non-uniform variation in winter temperature over East Asia. Atmos Ocean Sci Lett 8:376–382
Li S, He S, Li F, Wang H (2018) Simulated and projected relationship between the East Asian winter monsoon and winter Arctic Oscillation in CMIP5 models. Atmos Ocean Sci Lett 11:417–424
Lind S, Ingvaldsen RB, Furevik T (2018) Arctic warming hotspot in the northern Barents Sea linked to declining sea-ice import. Nat Clim Change 8:634–639
Liu J, Curry JA, Wang H, Song M, Horton RM (2012) Impact of declining Arctic sea ice on winter snowfall. Proc Natl Acad Sci 109:4074–4079
Luo D, Xiao Y, Yao Y, Dai A, Simmonds I, Franzke CLE (2016) Impact of Ural blocking on winter warm Arctic-cold Eurasian anomalies. Part I: Blocking-induced amplification. J Clim 29:3925–3947
Luo B, Luo D, Wu L, Zhong L, Simmonds I (2017) Atmospheric circulation patterns which promote winter Arctic sea ice decline. Environ Res Lett 12:054017
Marsh DR, Mills MJ, Kinnison DE, Lamarque JF, Calvo N, Polvani LM (2013) Climate change from 1850 to 2005 simulated in CESM1 (WACCM). J Clim 26:7372–7391
McCusker KE, Fyfe JC, Sigmond M (2016) Twenty-five winters of unexpected Eurasian cooling unlikely due to Arctic sea-ice loss. Nat Geosci 9:838–842
Mori M, Watanabe M, Shiogama H, Inoue J, Kimoto M (2014) Robust Arctic sea-ice influence on the frequent Eurasian cold winters in past decades. Nat Geosci 7:869–873
Neale RB, Richter J, Park S, Lauritzen PH, Vavrus SJ, Rasch PJ, Zhang M (2013) The mean climate of the Community Atmosphere Model (CAM4) in forced SST and fully coupled experiments. J Clim 26:5150–5168
Ogawa F et al (2018) Evaluating impacts of recent Arctic sea ice loss on the northern hemisphere winter climate change. Geophys Res Lett. https://doi.org/10.1002/2017gl076502
Onarheim IH, Årthun M (2017) Toward an ice-free Barents Sea. Geophys Res Lett 44:8387–8395
Onarheim IH, Eldevik T, Årthun M, Ingvaldsen RB, Smedsrud LH (2015) Skillful prediction of Barents Sea ice cover. Geophys Res Lett 42:5364–5371
Outten SD, Esau I (2012) A link between Arctic sea ice and recent cooling trends over Eurasia. Clim Change 110:1069–1075
Overland JE, Miletta Adams J, Bond NA (1999) Decadal variability of the Aleutian Low and its relation to high-latitude circulation*. J Clim 12:1542–1548
Overland JE, Wood KR, Wang M (2011) Warm Arctic-cold continents: climate impacts of the newly open Arctic Sea. Polar Res 30:157–171
Overland J, Francis JA, Hall R, Hanna E, Kim SJ, Vihma T (2015) The melting Arctic and midlatitude weather patterns: are they connected? J Clim 28:7917–7932
Panagiotopoulos F, Shahgedanova M, Hannachi A, Stephenson DB (2005) Observed trends and teleconnections of the Siberian high: a recently declining center of action. J Clim 18:1411–1422
Reynolds RW, Smith TM, Liu C, Chelton DB, Casey KS, Schlax MG (2007) Daily high-resolution-blended analyses for sea surface temperature. J Clim 20:5473–5496
Screen JA, Francis JA (2016) Contribution of sea-ice loss to Arctic amplification is regulated by Pacific Ocean decadal variability. Nat Clim Change 6:856–860
Screen JA, Simmonds I (2010) The central role of diminishing sea ice in recent Arctic temperature amplification. Nature 464:1334–1337
Screen JA, Deser C, Simmonds I (2012) Local and remote controls on observed Arctic warming. Geophys Res Lett 39:L10709
Screen JA et al (2018) Consistency and discrepancy in the atmospheric response to Arctic sea-ice loss across climate models. Nat Geosci 11:155–163

Shindell D, Faluvegi G (2009) Climate response to regional radiative forcing during the twentieth century. Nat Geosci 2:294–300
Smedsrud LH et al (2013) The role of the Barents Sea in the Arctic climate system. Rev Geophys 51:415–449
Sorokina SA, Li C, Wettstein JJ, Kvamstø NG (2016) Observed atmospheric coupling between Barents Sea ice and the warm-Arctic cold-Siberian anomaly pattern. J Clim 29:495–511
Sun L, Perlwitz J, Hoerling M (2016) What caused the recent "warm Arctic, cold continents" trend pattern in winter temperatures? Geophys Res Lett 43:5345–5352
Sung M-K, Kim S-H, Kim B-M, Choi Y-S (2018) Interdecadal variability of the warm Arctic and cold Eurasia pattern and its North Atlantic origin. J Clim 31:5793–5810
Takaya K, Nakamura H (2001) A formulation of a phase-independent wave-activity flux for stationary and migratory quasigeostrophic eddies on a zonally varying basic flow. J Atmos Sci 58:608–627
Takaya K, Nakamura H (2005) Mechanisms of intraseasonal amplification of the cold Siberian high. J Atmos Sci 62:4423–4440
Vavrus SJ (2018) The influence of Arctic amplification on mid-latitude weather and climate. Curr Clim Change Rep 4:238–249
Wang S, Liu J (2016) Delving into the relationship between autumn Arctic sea ice and central–eastern Eurasian winter climate. Atmos Ocean Sci Lett 9:366–374
Wang B, Wu Z, C-p Chang, Liu J, Li J, Zhou T (2010) Another look at interannual-to-interdecadal variations of the East Asian winter monsoon: the northern and southern temperature modes. J Clim 23:1495–1512
Woods C, Caballero R (2016) The role of moist intrusions in winter Arctic warming and sea ice decline. J Clim 29:4473–4485
Wu B, Wang J (2002) Possible impacts of winter Arctic Oscillation on Siberian High, the East Asian winter monsoon and sea–ice extent. Adv Atmos Sci 19:297–320
Xu X, He S, Li F, Wang H (2018a) Impact of northern Eurasian snow cover in autumn on the warm Arctic–cold Eurasia pattern during the following January and its linkage to stationary planetary waves. Clim Dyn 50:1993–2006
Xu X, Li F, He S, Wang H (2018b) Sub-seasonal reversal of East Asian surface temperature variability in winter 2014/2015. Adv Atmos Sci 35:737–752
Yang S, Lau KM, Kim KM (2002) Variations of the East Asian jet stream and Asian-Pacific-American winter climate anomalies. J Clim 15:306–325
Yao Y, Luo D, Dai A, Simmonds I (2017) Increased quasi stationarity and persistence of winter Ural blocking and Eurasian extreme cold events in response to Arctic warming. Part I: insights from observational analyses. J Clim 30:3549–3568
Zhu Y, Wang H, Wang T, Guo D (2018) Extreme spring cold spells in North China during 1961–2014 and the evolving processed. Atmos Ocean Sci Lett 11:432–437